Low-energy electron diffraction and ultraviolet photoemission spectroscopy study of (1 x 1) TiO_2 (110)

Erica T. Shen, Nancy Yu, Dr. Kenneth T. Park

Abstract— **Ar^+ sputtered and annealed TiO_2(110) was examined with ultraviolet photoemission spectroscopy (UPS) and low-energy electron diffraction (LEED). Ag(111) provided the baseline to calibrate the LEED data, while polycrystalline Au was utilized to calibrate the UPS data. Experimental LEED I(V) curves of TiO_2(110) were compared to published data, while the LEED pictures were used in dynamic determination of the symmetry and lattice constants of TiO_2(110). UPS was used to determine the work function of TiO_2(110). Lattice constants of a_1 = 3.0506 Å and a_2 = 7.1622 Å and a work function of 5.40 eV were determined for the rutile TiO_2(110)-(1 x 1) surface.**

***Index Terms*—LEED, UPS, TiO_2(110), Ag(111), I(V) curves, (1 x 1) reconstruction**

I. INTRODUCTION

Titanium dioxide is an extensively investigated compound with many applications, such as catalysis [1-3], gas sensing, white pigmentation, corrosion-protection, optical coating, ceramics, and electrical devices [4]. To be able to influence properties important to such applications, the clean surface structure of titanium dioxide must be well-understood, as all such applications involve the reactions on the surface of titanium dioxide. Studies of TiO_2(110) and other metal-oxide surfaces indicate that surface structure differs highly from that of the bulk [5], which has been well known and reviewed for decades. However, the surface structure remains under debate, especially that of the reconstruction (1 x 2) [6-11], as reconstructions are heavily influenced by sample preparation methods [4, 12]. Reconstruction is the movement of surface atoms into structures having different periodicity and/or symmetry than that of the bulk. Various tools, such as scanning tunneling microscopy (STM) [12-19], X-ray photoelectron spectroscopy (XPS) [20-22], Auger electron spectroscopy (AES) [20], low-energy electron diffraction (LEED) [23, 24], and ultraviolet photoemission spectroscopy (UPS) [17, 25-27] have been utilized to discern not only the atomic structure of titanium oxide, but also rearrangements and relaxations produced by adsorbates, deliberate perturbations, or preparation.

In this study, LEED and UPS have been utilized to observe an Ar^+ sputtered and annealed "clean" sample of rutile TiO_2(110). An Ag(111) sample was used as a baseline for calculations of TiO_2(110) LEED data, due to its bulk-like stability and well-reviewed status. A polycrystalline sample of Au was used as a baseline for calculations of TiO_2(110) UPS data, due to the high stability of Au, a noble metal.

II. EXPERIMENTAL

Materials

TiO_2(110), of the rutile polymorph, is the most widely studied surface of titanium dioxide. The stability of the (110) surface, as well as wide availability of high-quality samples, usually prepared by epitaxial polishing, makes it an excellent material for study [28]. The crystal structure is tetragonal, the unit cell consisting of six oxygen atoms surrounding a titanium atom in a slightly distorted octahedral configuration [4]. Depending on sample preparation conditions, a (1 x 2) or (1 x 1) reconstruction of the sample can be observed.

Ag(111) is a highly stable surface of Ag, having a bulk-terminated surface structure [29]. The crystal has a face-centered cubic structure, while the (111) face has an experimentally determined nearest neighbor distance of a = 2.89 Å [16]. The work function of Ag(111) is 4.70 eV [30] Using these well-reviewed values for instrument calibration, the properties of TiO_2(110) were determined.

Instrumentation, Theory, and Calculations

Experimentation was carried out in ultra-high vacuum, due to high scattering cross sections that cause a sample to become rapidly contaminated in non-vacuum as the sample is bombarded by foreign particles. Ultra-high vacuum (~10^{-10} torr) not only reduces the frequency of impacts, keeping the surface "clean", but permits a large enough mean free path for detection of particle surface probes, such as diffracted electrons [31].

LEED

LEED, or low energy electron diffraction, is a tool for surface structure study first proposed in 1927 by Davisson and Germer during experiments demonstrating the wave-particle nature of electrons . Interest in the tool waned at this point in time due to lack of UHV (leading to constant contamination of

Final draft completed Aug. 6th 2009. Work sponsored by the National Science Foundation and Baylor University.

samples to be examined) and an inability to penetrate into the core levels of a sample. In the 1960s and 70s, however, interest was revived once more as UHV became available, as well as LEED's ability to probe the surface structure in detail with low perturbation. The instrument, a rear-view LEED apparatus, consists of an electron gun, a phosphorous screen, and focusing grids. A CCD camera is used to take pictures of the LEED screen [32, 33].

LEED operates through the concept of elastic electron diffraction. The de Broglie wavelength $\lambda = \hbar / p$ for low energy electrons corresponds well with typical crystal lengths, and therefore allows for diffraction to occur. Electrons fired by the electron gun behave as a wave and are elastically diffracted by areas of high potential, namely, the surface atoms. This elastic diffraction causes electrons to hit the phosphorous screen in a regular pattern, exciting the phosphor to glow. Pictures are taken of the LEED screen during data collection, for later analysis.

Taking a computational view, the motion of the incident electron can be described by vector $\vec{k}$. Through elastic scattering, the vector $\vec{k}'$ is obtained as the electron diffracts off the surface at an angle. As the scattering is elastic, energy is conserved ($E = E'$). These vectors are unique, but equal in magnitude ($\left|\vec{k}\right| = \left|\vec{k}'\right|$).

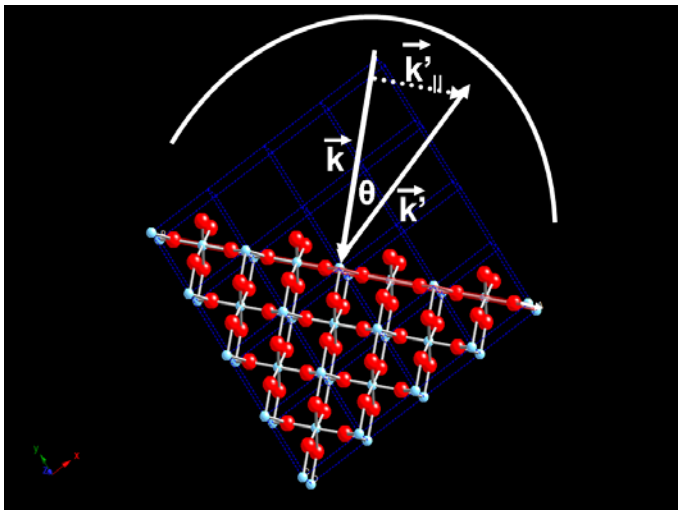

Fig. 1. Diagram of the elastic scattering of electrons off the surface of TiO_2(110). The arc represents the LEED phosphorescent screen. This diagram is not to scale.

The incident electron vector $\vec{k}$ does not have a parallel component, as it is directed perpendicular to the sample surface. However, the diffracted electron wave $\vec{k}'$ has the parallel component $\vec{k}'_{\parallel}$ and the perpendicular component $\vec{k}'_{\perp}$. The parallel component $\vec{k}'_{\parallel}$ is the reciprocal lattice vector (which describes the allowed modes of the crystal surface), which has the value:

$$\vec{k}'_{\parallel} = n\frac{2\pi}{a} \tag{1}$$

where n is the order of diffraction. As indicated in Fig. 1, the relationship between the vectors can be expressed as:

$$\sin\theta = \frac{\vec{k}'_{\parallel}}{\vec{k}'} = n\frac{2\pi}{a\vec{k}'} \tag{2}$$

The quantum definition of the energy of an electron is:

$$E = \frac{\left(\hbar\vec{k}'\right)^2}{2m_e} \tag{3}$$

where ħ is Planck's constant, m_e is the mass of the electron, and $\vec{k}'$ is the wave number of the elastically scattered electron. Through rearrangement and substitution, it can be shown that:

$$\vec{k}' = \sqrt{\frac{2m_e E}{\hbar^2}} \approx 0.5123\sqrt{E} \tag{4}$$

where E is in units of eV, and $\vec{k}'$ is in units of in units of Å. Therefore, substituting into the diffraction equation for the final time:

$$\sin\theta = n\frac{2\pi}{a(0.5123\sqrt{E})} \tag{5}$$

Through this equation, it is clear that with increasing energy, the angle of diffraction decreases. Thus, as LEED data is taken over a voltage range, the diffraction spots on the phosphorous screen move inward, allowing for more orders to be viewed. Knowing the radius of the LEED phosphorous screen as 2.75 cm, and utilizing the lattice constant of Ag(111), one can calculate the distance from the screen to the sample. Taking into account averaging across orders of diffraction, the value of $\sin\theta$ is determined as a constant. Thus, only E is the only independent variable. Rearranging the equation provides:

$$a = n\frac{2\pi}{\sin\theta(0.5123\sqrt{E})} \tag{6}$$

CCD pictures of the LEED phosphorous screen are examined manually to find the energies at which diffraction spots of various orders appear at the edge of the screen – these energies are used as *E*. Thus from LEED data can the lattice constant of a sample be determined. However, TiO_2 (110) is a rectangular unit cell (in 2D), and thus has two different lattice constants.

Other data that can be determined by LEED include surface symmetry (by evaluation of the 2D pictures taken by the CCD camera), also known as qualitative analysis, and the distance between surface planes (by analysis of intensity vs. voltage, or I(V) curves), known as quantitative analysis, or dynamical LEED analysis.

Analysis of LEED I(V) curves is considered a multiparameter problem, in which all unknowns are determined in a simultaneous fit. This has caused valid concern over the accuracy and sensitivity of LEED, but comparisons of cases where a surface's composition is well known from another source show that LEED provides accurate data, possibly even exceeding expectations [20]. LEED allows one to find the full surface structure by first

obtaining reliable data, calculating accurate intensities for a probable structural model, and then finally calculating the correct structure by variation of model parameters [34]. Agreement between calculated theoretical I(V) curves and experimental I(V) curves is determined by the Pendry R-factor [35].

UPS

Ultraviolet photoelectron spectroscopy, or UPS, is a method of determining the electronic structure of a sample. Through photoemission [36], photons excite electrons from orbitals into the vacuum, where they are collected by a hemispherical detector. The beams are accelerated and focused during their travel, eventually striking the detector.

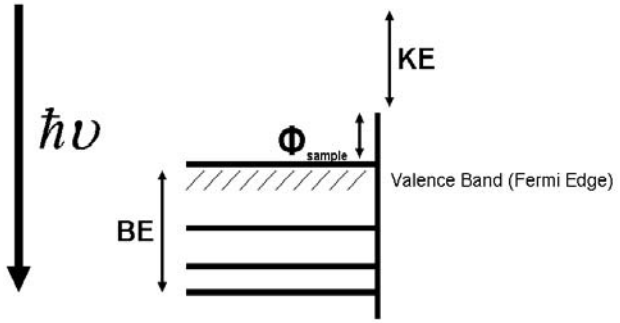

Fig. 2. Diagram of photoemission, through which a photon excites electrons from the orbitals of a sample.

The energy of a photon can be described quantitatively as $E = \hbar\upsilon$, where υ is the frequency of the photon. Based on Fig. 2, it can be seen that:

$$\hbar\upsilon = KE + BE + \Phi_{sample} \quad (7)$$

where KE is the energy of the electron initially excited from the sample, BE is the binding energy of the electron (energy required to move the electron from the orbital level to the Fermi/highest orbital level), Φ_{sample} is the work function of the sample (energy required to excite an electron from the Fermi/highest orbital level into vacuum).

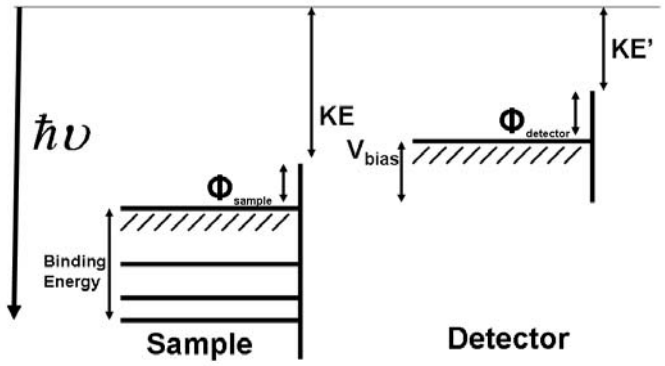

Fig. 3. Diagram representing UPS. The detector is biased from the Fermi edge of the sample. KE' is the energy observed by the detector. KE' ≠ KE. The shaded regions represent the valence band (Fermi edge).

Fig. 3 describes the setup of UPS, showing the electron orbital levels of the sample and detector during scanning. One now derives that the kinetic energy of the detector is:

$$KE' = KE + \Phi_s - \Phi_d - V_{bias} \quad (8)$$

where KE' is the energy observed by the detector, V_{bias} is the voltage bias applied to the detector, and Φ_d is the work function of the detector. When $KE = 0$, representing the electrons coming from the deepest level that the UPS can probe (or, however, from multiple-scattered electrons, which are a source of error), the secondary electron cutoff (SEC), then:

$$KE' = (\Phi_s - \Phi_d) - V_{bias} \quad (9)$$

Therefore:

$$\Phi_d = \Phi_s - KE' - V_{bias} \quad (10)$$

Once the work function of the detector has been obtained, the equation may be rearranged to:

$$\Phi_s = \Phi_d + KE' + V_{bias} \quad (11)$$

Thus can the work function of the sample be obtained.

III. Procedure

First, the vacuum chamber underwent a 48-hour baking period, until the pressure reached 10^{-10} torr. The samples were then cleaned through Ar^+ gas sputtering, then annealing. However, the cleaning parameters differed between samples. During sputtering Ag(111) obtained a current of ~5.6-6.1 μA and a voltage of 3000V. Ag(111) was annealed at ~480 C° by e-beam bombardment of the sample holder. Temperature was monitored by a chromel-alumel thermocouple. Sputtering and annealing lasted 10-20 minutes each, with time decreasing as more cycles were performed to prevent excessive reconstruction of the sample. Ag(111) was then allowed to cool to <100 C°.

For TiO_2(110), a sample current of ~0.8-1.0 μA and a voltage of 3000V was applied during sputtering, for 10-20 minutes. TiO_2(110) was annealed at ~600 °C. The increasing/decreasing rate of heating was carefully controlled.. Annealing lasted 15 minutes, decreased to 10 minutes in cleaning cycles prior to data collection. TiO_2(110) was then allowed to cool to <100 °C.

LEED data was taken over 65-210 eV for Ag(111), and 35-165 eV for TiO_2. I(V) curves were extracted using a Labview program written by Trinity Ellis [37]. Three passes of data were taken for each sample; the sample was not cleaned in between passes.

In taking UPS data, the UV He I source, producing photoemission energy of 21.2 eV, was used. High resolution and low magnification scans of 20 passes were run on TiO_2(110) and Ag(111) to find the SEC. A bias of -11V was applied during scanning to avoid stray low-energy electrons

IV. Results

A) *LEED*

(10) and (01) curves were analyzed for Ag(111), utilizing one pass of data. (10), (01), (11), and (02) curves were analyzed for TiO_2(110), utilizing three passes of data. The second pass of data is graphed for the (10), (01), and (11) curves, however, the first pass of data is graphed for the (02) curve. All data was normalized with RAMP values specific to each pass. RAMP values correct for errors generated in the CCD camera by imperfect pixels in the CCD array. Fig. 4 is a

CCD picture of the LEED phosphor screen at 105 eV, revealing a (1 x 1) reconstruction pattern, as previously observed [10], showing periodicity in the [0 0 1] and [1 -1 0] directions.

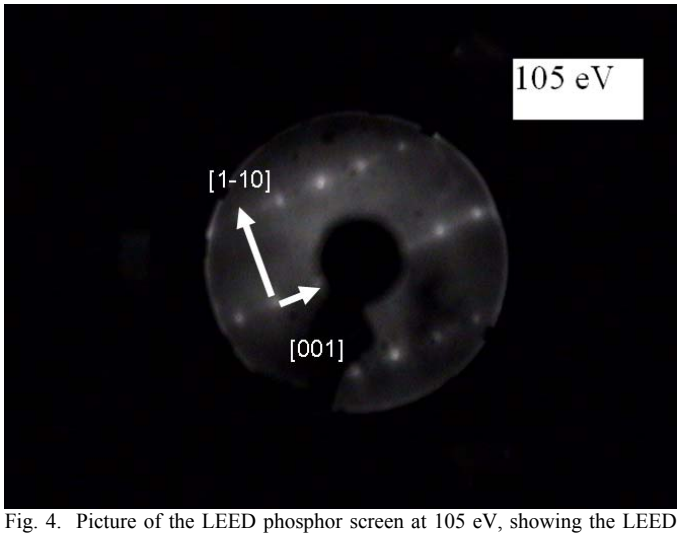

Fig. 4. Picture of the LEED phosphor screen at 105 eV, showing the LEED pattern for TiO_2(110). The (1 x 1) periodicity of the sample can be clearly seen, as shown by LEED spots emerging along the [001] and [1-10] directions.

For the 10 I(V) Ag(111) curve, averaging of maxima locations gives the following peak positions: 75 eV, 120 eV, 131 eV, and 194.5 eV. For the 01 I(V) Ag(111) curve, averaging of maxima locations gives the following peak positions: 115.5.eV, 143.5 eV, 167 eV, 187.5 eV.

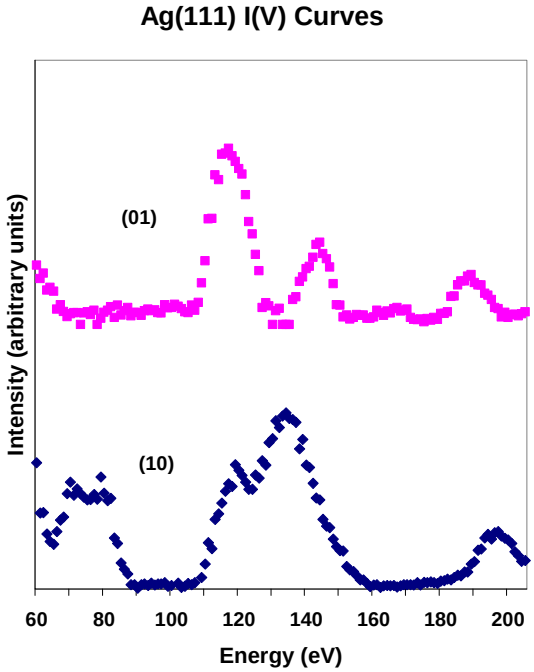

Fig. 5. Diagram representing the (10) and (01) I(V) curves of Ag(111).

For the (11) I(V) TiO_2(110) curve, averaging of maxima locations gives the following peak positions: 106 eV, 121.3 eV, 142.6 eV. For the (10) I(V) TiO_2(110) curve, averaging of maxima locations gives the following peak positions: 63 eV, 80.3 eV, 101.3 eV, 117.6 eV. For the (01) I(V) TiO_2(110) curve, averaging of maxima locations gives the following peak positions: 47 eV, 71 eV, 94 eV, 112.6 eV, and 130.3 eV. For the (02) I(V) TiO_2(110) curve, peak positions are: 79 eV, 104 eV, 123 eV.

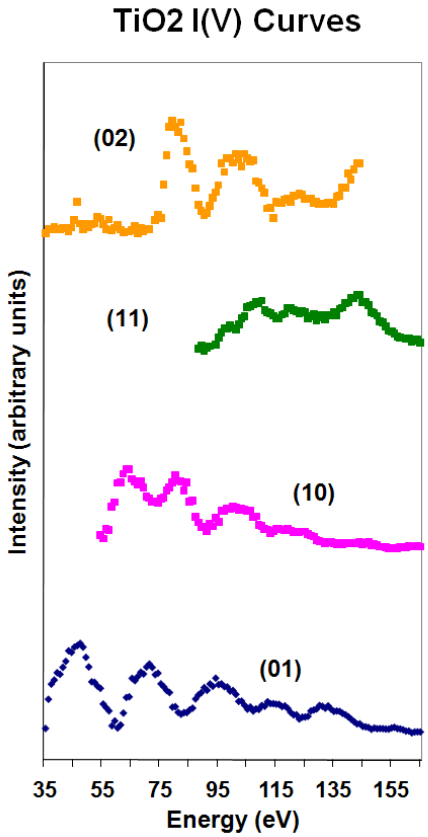

Fig. 6. Diagram representing the (10), (01), (11), and (02) I(V) curves of TiO_2(110).

For all scans, the maxima peaks became less distinct as time elapsed due to recontamination of the samples.

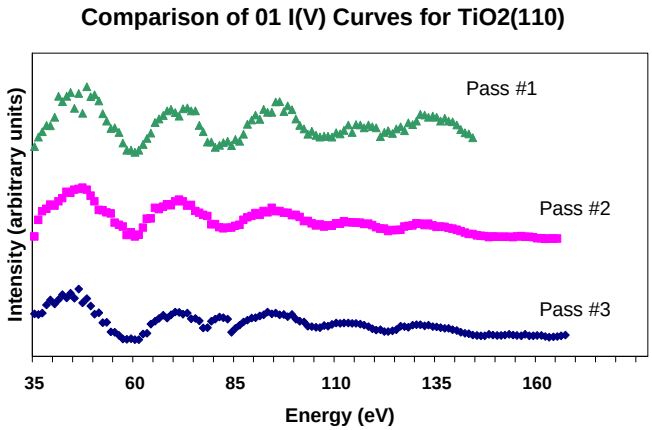

Fig. 7. This diagram depicts the increased contamination of the sample with time.

Using the equation derived in the Experimental section, the lattice constants of TiO_2 are calculated to be a_1 = 3.0506 Å, a_2 = 7.1622 Å.

B) *UPS*

Using the scans of secondary electron cutoff of polycrystalline Au, the kinetic energy observed by the detector is found to be 13 eV.

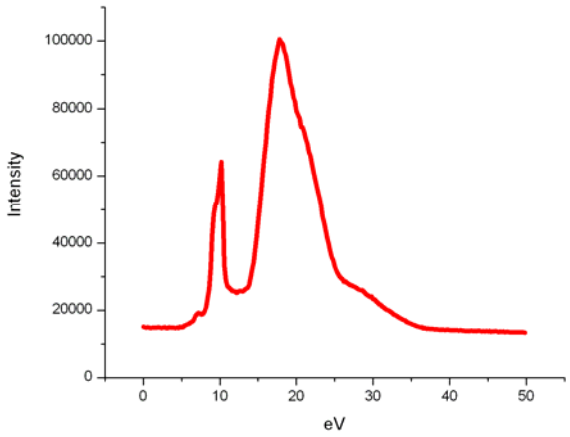

Fig. 8. The secondary electron cutoff scan of the polycrystalline sample of Au.

Utilizing the equations derived in the introduction, the work function of the detector is calculated to be 2.70 eV. For TiO_2's secondary electron cutoff, the kinetic energy is found to be 13.7 eV.

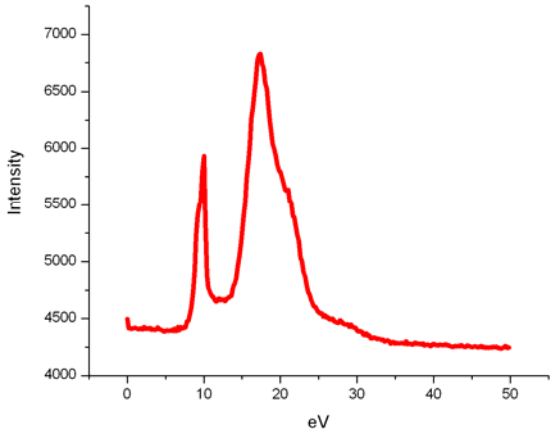

Fig. 9. The secondary electron cutoff scan of TiO_2(110).

Therefore, utilizing the same equation, the work function of TiO_2 is found to be 5.40 eV.

V. Discussion/Analysis

Ag(111) I(V) curves show excellent correlation to that of the Stony Brook LEED group [38].

There have been few LEED quantitative analysis of the clean rutile TiO_2(110) (1 x 1) reconstruction, with most attention focused on the behavior of adsorbates exhibiting (1 x 1) structure upon the TiO_2(110) surface [24] or that of the (1 x 2) reconstruction. Lindsay *et. al*, however, performed such a study, combined with theoretical modeling of the TiO_2(110) (1 x 1) reconstruction compared to gathered experimental data [39]. I(V) data collected in this study shows good correlation to the theoretical I(V) curves of (10), (11), and (02) reported by Lindsay *et. al*, confirming that the structure is indeed (1 x 1). Lindsay *et. al* reports an R_p factor of 0.64 for the best-fit structure.

Comparison of the obtained experimental data to the theoretical curves (versus that of the experimental data obtained in [39]) provides a much closer fit to theory than previously reported. In the (11) curve, the features are sharper than predicted in theory, but the "valley" between 106 eV and 142.6 eV is apparent. The (10) curve shows an excellent fit, resolving the three "shoulder" peaks that theory predicts, then tapering off into two minor peaks accordingly. The (02) curve captures the relative intensities of the peaks predicted in theory very well, again resolving the "shoulder" peaks. There is not sufficient data available in the theoretical or experimentally reported (01) curve to determine if our data correlates well; regardless, visual inspection clearly indicates that we have obtained well defined peaks for various energies.

Curiously enough, the (1 x 1) reconstruction was obtained at a much lower annealing temperature than previously reported. As temperature dependence has been shown for preferential reconstruction (1 x 2) at lower temperatures, it is most likely that the sample was not highly reduced by the preparation methods in this study. Reduced samples have been shown to preferentially reconstruct to (1 x 2), with an inability to reconstruct to (1 x1) after loss of enough bulk oxygen [23].

The value obtained for the lattice constant along the [1 -1 0] direction shows excellent correlation with reported values [10, 40]. The value obtained for the lattice constant along the [0 0 1] direction, however, is slightly higher than previously reported values, as 7.1622 Å is ~10% higher than the reported value of 6.49 Å [10, 40, 41]. The work function obtained in this study is also on the high-end range of previously reported work functions ranging amongst 4.24 eV [13], 5.32 eV or 5.06 eV [27], and from 4.6-5.5 eV [26]. However, sample preparation methods have been shown to highly affect work function. It has also been shown that argon sputtering and annealing preparation procedures create point defects on the surface of the sample, which would cause a rise in work function. Sputtering and annealing can also cause a sample to become reduced due to preferential sputtering of oxygen [27, 42, 43]. Reduction of a sample will also increase the work function.

IV. Conclusion

LEED and UPS studies of the rutile TiO_2(110) surface cleaned in annealing and sputtering have yielded results characterizing a (1 x 1) reconstruction of the clean surface. Our results show excellent correlation with the previously reported "best-fit" model of the rutile TiO_2(110) surface, better than previously reported experimental data. Lattice constants of a_1 = 3.0506 Å and a_2 = 7.1622 Å have been determined for rutile TiO_2(110)-(1 x 1) surface. A work function of 5.40 eV has also been determined for the rutile TiO_2(110)-(1 x 1) surface. For future work, as only dynamical

LEED has been performed in this study, a theoretical LEED study should be performed for comparison.

ACKNOWLEDGMENTS

Work was sponsored by the National Science Foundation and Baylor University. Baylor University is greatly thanked for the use of their facilities. Many thanks to David Katz and Ke "Zach" Zhe for technical assistance. The authors would also like to thank Dr. Lorin Matthews and Dr. Truell Hyde, the coordinators of the Baylor REU program.

REFERENCES

[1] A. Fujishima, X. Zhang and D. A. Tryk. (2008, 12/15). TiO2 photocatalysis and related surface phenomena. Surface Science Reports 63(12), pp. 515-582.

[2] A. Imanishi, H. Suzuki, N. Ohashi, T. Ohta and Y. Nakato. (2008, 2/15). Dye-sensitized photocurrents and adsorption properties of merocyanine dye at atomically flat rutile (1 1 0) and (1 0 0) TiO2 surfaces. Inorg. Chim. Acta 361(3), pp. 778-782.

[3] Ralf Bechstein, Mitsunori Kitta, Jens Schutte, Hiroshi Onishi and Angelika Kuhnle, "The effects of antimony doping on the surface structure of rutile TiO2(110)," Nanotechnology, vol. 20, pp. 7, 2009.

[4] U. Diebold. (2003, 1). The surface science of titanium dioxide. Surface Science Reports 48(5-8), pp. 53-229.

[5] G. A. Somorjai and J. Y. Park. (2009, 6/1). Concepts, instruments, and model systems that enabled the rapid evolution of surface science. Surf. Sci. 603(10-12), pp. 1293-1300.

[6] I. D. Cocks, Q. Guo and E. M. Williams. (1997, 11/18). ESDIAD studies of the structure of TiO2(110)(1 × 1) and (1 × 2) surfaces and interfaces in conjunction with LEED and STM. Surf. Sci. 390(1-3), pp. 119-125.

[7] K.T. Park, M.H. Pan, V. Meunier and E.W. Plummer. (2006, Surface reconstructions of TiO2(110) driven by suboxides. PRL 96

[8] M. Blanco-Rey, J. Abad, C. Rogero, J. Méndez, M. F. López, E. Román, J. A. Martín-Gago and P. L. de Andrés, "LEED-IV study of the rutile TiO2(110)-1x2 surface with a Ti-interstitial added-row reconstruction," Phys. Rev. B, vol. 75, 2007.

[9] M. Blanco-Rey, J. Abad, C. Rogero, J. Mendez, M.F. Lopez, J.A. Martin-Gago and P. L. de Andrés, "Structure of Rutile TiO2(110)-(1 x 2): Formation of Ti2O3 Quasi-1D Metallic Chains," Physical Review Letters, vol. 96, 2006.

[10] H. Onishi and Y. Iwasawa. (1994, 6/20). Reconstruction of TiO2(110) surface: STM study with atomic-scale resolution. Surf. Sci. 313(1-2), pp. L783-L789.

[11] R. Lindsay, S. Tomic, A. Wander, M. Garcia-Mendez and G. Thornton, "Low Energy Electron Diffraction Study of TiO2(110)(2 x 1)-[HCOO]-," J. Phys. Chem. C, vol. 112, pp. 14154-14157, 2008.

[12] E. Asari and R. Souda. (2002, 6/5). Atomic structures of TiO2(1 1 0) surface between p(1×1) and p(1×2) studied by scanning tunneling microscopy. Appl. Surf. Sci. 193(1-4), pp. 70-76.

[13] Akihito Imanishi, Etsushi Tsuji and Yoshihiro Nakato, "Dependence of the Work Function of TiO2(Rutile) on Crystal Faces, Studied by a Scanning Auger Microprobe," J. Phys. Chem. C, vol. 111, pp. 2128, 2007.

[14] Q. Guo and E. M. Williams. (1999, 8/2). The effect of adsorbate–adsorbate interaction on the structure of chemisorbed overlayers on TiO2(110). Surf. Sci. 433-435pp. 322-326.

[15] Hiroshi Uetsuka, Akira Sashara and Hiroshi Onishi, "Topography of the Rutile TiO2(110) Surface Exposed to Water and Organic Solvents," Langmuir, vol. 20, pp. 4782, 2004.

[16] Markus Lackinger, Stefan Griessl, Wolfgang M. Heckl and Michael Hietschold, "Coronene on Ag(111) Investigated by LEED and STM in UHV," J. Phys. Chem. B, vol. 106, pp. 4482, 2002

[17] T. Minato, T. Susaki, S. Shiraki, H. S. Kato, M. Kawai and K. Aika. (2004, 9/20). Investigation of the electronic interaction between TiO2(1 1 0) surfaces and Au clusters by PES and STM. Surf. Sci. 566-568(Part 2), pp. 1012-1017.

[18] O. Bondarchuk and I. Lyubinetsky, "Preparation of TiO2(110)-(1x1) surface via UHV cleavage: A scanning tunneling microscopy study," Review of Scientific Instruments, vol. 78, 2007.

[19] Yasuhiro Iwasawa, Hiroshi Onishi and Ken-ichi Fukui, "In situ STM study of surface catalytic reactions on TiO2(110) relevant to catalyst design," Topics in Catalysis, vol. 14, pp. 163, 2001.

[20] V. Blum, L. Hammer, W. Meier and K. Heinz. (2001, 8/1). Quantification of substitutional disorder and atomic vibrations by LEED – the role of parameter correlations. Surf. Sci. 488(1-2), pp. 219-232.

[21] L. Wang, D. R. Baer, M. H. Engelhard and A. N. Shultz. (1995, 12/30). The adsorption of liquid and vapor water on TiO2(110) surfaces: The role of defects. Surf. Sci. 344(3), pp. 237-250.

[22] L. P. Zhang, M. Li and U. Diebold. (1998, 9/3). Characterization of Ca impurity segregation on the TiO2(110) surface. Surf. Sci. 412-413pp. 242-251.

[23] K. F. McCarty and N. C. Bartelt. (2003, 3/10). The 1×1/1×2 phase transition of the TiO2(1 1 0) surface—variation of transition temperature with crystal composition. Surf. Sci. 527(1-3), pp. L203-L212.

[24] C. Su, J. -. Yeh, J. -. Lin and J. -. Lin. (2001, 1/15). The growth of Ag films on a TiO2(110)-(1×1) surface. Appl. Surf. Sci. 169-170pp. 366-370.

[25] E. Kroger, D. Sayago, F. Allegretti, M. Knight, M. Polcik, W. Unterberger, T. Lerotholi, K. Hogan, C. Lamont and D. Woodruff. (2007, Photoelectron diffraction investigation of the structure of the clean TiO2(110)(1x1) surface. Physical Review. B, Condensed Matter and Materials Physics vol.75(no.19), Available: http://d.wanfangdata.com.cn/NSTLQK_NSTL_QK14239747.aspx

[26] Michela Della Negra, Nanna Meyland Nicolaisen, Zheshen Li and Preben Juul Moller, "Study of the interactions between the overlayer and the substrate in the early stages of palladium growth on TiO2(110)," Surface Science, vol. 540, pp. 117, 2003.

[27] Victor E. Henrich, "Ultraviolet photoemission studies of molecular adsorption on oxide surfaces," Progress in Surface Science, vol. 9, pp. 143, 1979.

[28] Victor E. Henrich, "The surface of metal oxides," Rep. Prog. Phys., vol. 48, pp. 1481, 1985.

[29] E. A. Soares, V. B. Nascimento, V. E. de Carvalho, C. M. C. de Castilho, A. V. de Carvalho, R. Toomes and D. P. Woodruff. (1999, 1/4). Structure determination of Ag(111) by low-energy electron diffraction. Surf. Sci. 419(2-3), pp. 89-96.

[30] David R. Lide, Ed., *Handbook of Chemistry and Physics*, 76th ed. New York: CRC Press, 1995.

[31] G. A. Somorjai and J. Y. Park. (2009, 6/1). Concepts, instruments, and model systems that enabled the rapid evolution of surface science. Surf. Sci. 603(10-12), pp. 1293-1300.

[32] John W. May, "Discovery of Surface Phases by Low Energy Electron Diffraction (LEED)," Advances in Catalysis, vol. 21, pp. 151, 1970.

[33] R. Roucka, J. Jiruse and T. Sikola. (2002, 4/19). Spot intensity processing in LEED images. Vacuum 65(2), pp. 121-126.

[34] K. Heinz, M. Kottcke, U. Löffler and R. Döll. (1996, 6/20). Recent advances in LEED surface crystallography. Surf. Sci. 357-358pp. 1-9.

[35] J B Pendry, "Reliability factors for LEED calculations," J. Phys. C: Solid St. Phys., vol. 13, pp. 937, 1980.

[36] J. B. Pendry. (1976, 7/2). Theory of photoemission. Surf. Sci. 57(2), pp. 679-705.

[37] T. Ellis, "Heteroepitaxial Metallo-Phthalocyanine (MPc, M = Co, Ni, Cu) Thin Films on Gold: Atomic and Interfacial Electronic Structures," Ph. D. thesis, Baylor University, Waco, TX, United States of America, 2005.

[38] Stony Brook group, "The I(V) Data Repository," [Online]. Available: http://www.matscieng.sunysb.edu/ivdata/

[39] R. Lindsay, A. Wander, A. Ernst, B. Montanari, G. Thornton and N.M. Harrison, "Revisiting the Surface Structure of TiO2(110): A Quantitative low-Energy Electron Diffraction Study," Physical Review Letters, vol. 94, 2005.

[40] E. A. Akhadov, S. A. Safron, J.G. Skofronick, D. H. Van Winkle, F. A. Flaherty and Rifat Fatema, "Surface lattice dynamics of rutile TiO2(110) using helium atom surface scattering," Physical Review B, vol. 68, 2003.

[41] A. Sasahara, H. Uetsuka and H. Onishi. (2003, 4/1). Local work function of a rutile TiO2(1 1 0)-(1×1) surface observed by Kelvin probe force microscopy. Surf. Sci. 529(1-2), pp. L245-L250.

[42] L. Bugyi, A. Berkó, L. Óvári, A. M. Kiss and J. Kiss. (2008, 5/1). Enhanced dispersion and stability of gold nanoparticles on stoichiometric and reduced TiO2(1 1 0) surface in the presence of molybdenum. Surf. Sci. 602(9), pp. 1650-1658.

[43] R.H. Tait and R. V. Kasowski, "Ultraviolet photoemission and low-energy-electron diffraction studies of TiO2(rutile) (001) and (110) surfaces," Physical Review B, vol. 20, pp. 5178

Erica T. Shen (Baylor REU 2009) Born in Cincinnati, OH, on March 23, 1991, she has lived 18 years in West Virginia, recently moving to Houston, Texas. She attended George Washington High School in Charleston, WV, and graduated in the spring of 2009. She will begin her undergraduate studies in fall of 2009 at the University of California in Berkeley, CA, in the field of electrical engineering and computer science.

She participated in the 2008 Baylor HSSSRP under the guidance of Dr. Victor Land, working with CASPER upon dusty plasmas. She has also participated as a Student Fellow in the 2008 Earthwatch program, working at Los Alamos National Laboratory observing transient phenomena under the direction of Dr. Aimee Hungerford.